A model for numerical analysis of pressure leak-off response during hydraulic fracturing within naturally fractured formations

Un modèle pour analyse numérique de la réponse de fuite de pression lors de la fracturation hydraulique dans des formations naturellement fracturées

D.-J. Youn, D.V. Griffiths
Civil and Environmental Engineering, Colorado School of Mines, USA, dyoun@mines.edu

ABSTRACT: During hydraulic fracturing, pre-existing natural fractures may significantly affect the final fracture geometry. For a better understanding of the fracturing process, a pressure leak-off test data can be used to monitor the entire fracturing process including hydraulic fracture initiation, propagation and coalescence with pre-existing natural fractures. The main objective of this paper is to describe a novel numerical model for investigating pressure leak-off response during hydraulic fracturing. The model allows the fluid bottomhole pressure to be observed under different fracturing conditions. To achieve this, a hydro-mechanical coupled model based on an eXtended Finite Element Method (XFEM) is developed and applied. The mechanical behavior of the domain with discontinuities can be estimated without explicitly meshing the discontinuities as would be necessary in a traditional discrete fracture FE model. A sequential coupling scheme using Picard iteration is applied to the XFEM model to reproduce the hydro-mechanical coupling behavior during the hydraulic fracturing. The goal of this research is to improve the practical understanding of the influence of pre-existing fractures on pressure leak-off response during hydraulic fracture propagation.

RÉSUMÉ : Au cours de la fracturation hydraulique, les fractures naturelles préexistantes peuvent affecter de manière significative la géométrie finale de la fracture. Pour une meilleure compréhension du processus de fracturation, on peut utiliser des données de test de perte de pression pour surveiller l'ensemble du processus de fracturation, y compris l'initiation, la propagation et la coalescence des fractures hydrauliques avec des fractures naturelles préexistantes. L'objectif principal de cet article est de décrire un nouveau modèle numérique permettant d'étudier la réponse de fuite de pression lors de la fracturation hydraulique à l'aide d'unprogramme d'éléments finis couplés avancés. Le modèle permet d'observer la pression d'injection du fluide dans différentes conditions de fracturation . Pour ce faire, un modèle couplé hydro-mécanique basé sur une méthode des éléments finis étendus (XFEM) est développé et appliqué. Le comportement mécanique du domaine à discontinuités peut être estimé sans mapper explicitement les discontinuités comme cela serait nécessaire dans un modèle traditionnel de fractures discrète FE. Un schéma de couplage séquentiel utilisant l'itération de Picard est appliqué au modèle XFEM pour reproduire le comportement de couplage hydro-mécanique lors de la fracturation hydraulique. L'objectif de cette recherche est d'améliorer la compréhension pratique de l'influence des fractures préexistantes sur la réponse de fuite de pression pendant la propagation de fracture hydraulique.

KEYWORDS: eXtended Finite Element Method (XFEM), hydraulic fracturing, pressure leak-off, HM coupling analysis

1 INTRODUCTION

During hydraulic fracturing, the fluid bottomhole pressure is routinely monitored and recorded as of a pressure leak-off test to estimate the equivalent formation permeability of the stimulated zone of the reservoir. However, the technique may also be used to detect unexpected patterns of the hydraulic fracture propagations due to the possible uncertainties within the formation such as pre-existing natural fractures. Compared to the case with natural fractures, Fig. 1 presents a regular fluid pressure variation during a hydraulic fracturing process within a homogeneous and isotropic formation.

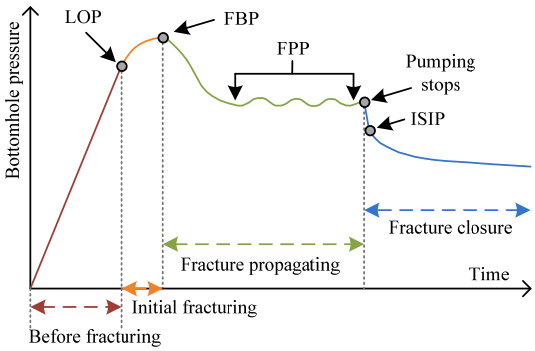

Figure 1. Pressure leak-off test data during a hydraulic fracturing treatment (Youn, 2016)

The bottomhole pressure initially builds up rapidly as the fracturing fluid is injected, and the surrounding rock expands elastically. When the injected fluid initiates a hydraulic fracture, the pressure deviates from the linear trend, and the point where this deviation occurs is known as the leak-off pressure (LOP). During the fracture propagation, both the fracture internal volume and permeability increase, and thus the bottomhole pressure decreases from the maximum bottomhole pressure (FBP) and remains relatively stable at the fracture propagation pressure (FPP). If the pumping stops, the fluid flows back, and the bottomhole pressure rapidly decreases to the instant shut-in pressure (ISIP). Later the pressure gradually drops to the reservoir pressure.

Compared to the ideal case described above, the pressure may noticeably differ during an actual hydraulic fracturing. The difference is mainly from the formation heterogeneity such as natural fractures in the formation. The natural fracture system not only causes a non-uniform stress distribution near the hydraulic fracture but also increases the internal volume of the fracture network so that the internal fluid pressure may present a sudden decrease when the hydraulic fracture intersects the natural fractures. Therefore, the pressure leak-off test data can be used to analyze the status of the hydraulic fracturing process in the deep underground. In this research, the bottomhole pressure variations during hydraulic fracturing within naturally fractured reservoirs are analyzed using a hydro-mechanical coupled eXtended Finite Element Method (XFEM) program.

2 HYDRO-MECHANICAL COUPLING XFEM MODEL

2 .1 *The eXtended Finite Element Method (XFEM)*

The XFEM was first developed based on a Partition of Unity Method (PUM) by Belytschko and Black (1999) and Moës et al. (1999). The relatively new technique has great potential for modeling fractures without a redundant remeshing process.

In this research, two different enrichment functions as shown in Fig. 2 are used to capture and represent two types of discontinuities such as fracture surface and tip. First, a fracture can be divided to the fracture surfaces showing opposite movement of the fracture aperture as shrinkage or dilation, and the tips presenting the fracture asymptotic field based on Westergaard's solution (Moës et al., 1999). In the XFEM, the displacements of the fracture surface and tip are then represented by Heaviside and Branch enrichment functions as shown in Eqs. 1 and 2. respectively (See Fig. 2).

$$H(\mathbf{x}) = \begin{cases} +1 & \phi(\mathbf{x}) \geq 0 \\ -1 & \phi(\mathbf{x}) < 0 \end{cases} \tag{1}$$

$$\left[\Phi_\gamma(\mathbf{x})\right]_{\gamma=1}^{4} = \left[\sqrt{r}\sin\frac{\theta}{2}, \sqrt{r}\cos\frac{\theta}{2}, \sqrt{r}\sin\theta\sin\frac{\theta}{2}, \sqrt{r}\sin\theta\sin\frac{\theta}{2}\right] \tag{2}$$

where $\phi(\mathbf{x})$ is the signed distance function measuring the minimum distance from the fracture to nodes **x**, and r and θ are the polar coordinates of the point **x** in the coordinate system centered on the tip of the fracture. The enrichment functions are from classical linear elastic fracture mechanics (LEFM) and represent the discontinuous displacement field around a fracture surface and the tips, respectively

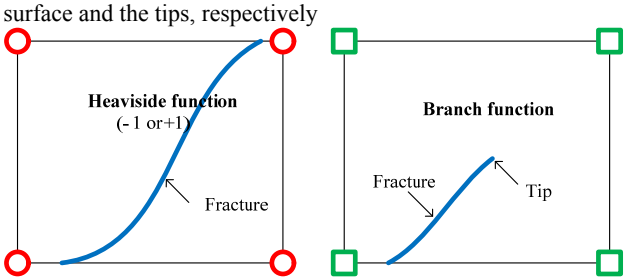

(a) Element divided by a fracture (b) Element containing a fracture tip

Figure 2. Enrichment functions (Youn, 2016)

The XFEM uses the local enrichment functions for approximate discontinuous fields, because the effects of the discontinuities are usually concentrated within limited local areas. Therefore, the enrichment function is only required within zones including discontinuities rather than enriching the whole domain of the system. Due to this characteristic, XFEM is able to improve the computation efficiency. To represent various displacement characteristics (e.g. fracture surfaces and tips), the general form of the XFEM displacement approximation is presented as in Eq. 3.

$$\mathbf{u}(\mathbf{x}) = \sum_{i=1}^{N} \mathcal{N}_i(\mathbf{x})\bar{\mathbf{u}}_i + \sum_{j=1}^{M_1} N_j(\mathbf{x}) f_1^{enr}(\mathbf{x})\bar{\mathbf{a}}_j + \sum_{k=1}^{M_2} N_k(\mathbf{x}) f_2^{enr}(\mathbf{x})\bar{\mathbf{b}}_k \tag{3}$$

where M_1 and M_2 are the different sets of nodes enriched by the functions, f_1^{enr} and f_2^{enr}, respectively, and N_i, N_j and N_k are finite element shape functions. The shape functions for the enrichment part are not necessarily the same as the shape functions for the continuous part (Dahi, 2009; Koei 2014). $\bar{\mathbf{a}}_j$ and $\bar{\mathbf{b}}_k$ are the nodal degrees of freedom vectors for the enrichment functions, f_1^{enr} and f_2^{enr} respectively.

2 .2 *Hydro-Mechanical Coupling Scheme*

This section presents enhancements to the XFEM program to integrate fracture propagation into a hydro-mechanical (HM) coupling system. Due to the sequential coupling scheme used in this research, 1D and 2D finite element meshes are separately created for the calculations of the hydraulic pressure and fracture displacement, respectively. For each time step, the 1D fluid pressure calculation and 2D XFEM are repeated sequentially until the fracture aperture and fluid pressure converge. Once the fluid pressure yields the stress intensity factor (SIF), K_I exceeding the pre-defined mode I fracture toughness, K_{IC}, an additional fracture length is added at the existing fracture tip providing the fracture volume change. The overall coupling program algorithm is presented in Fig. 3.

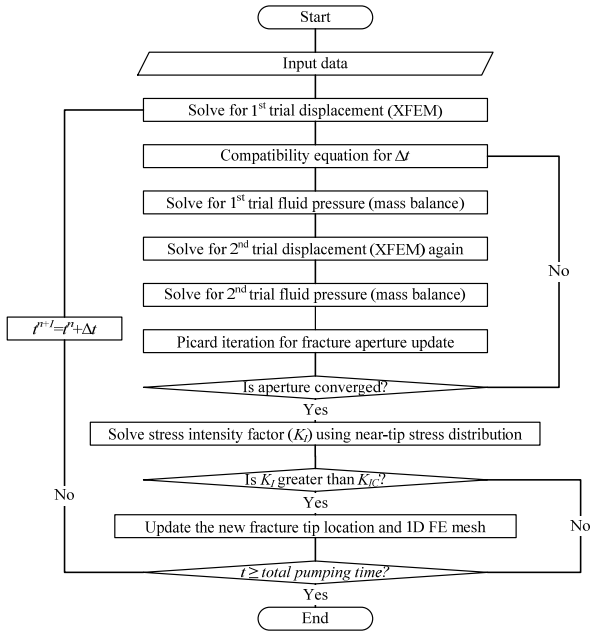

Figure 3. Flowchart for the coupling algorithm of a hydraulic fracture simulation

For fluid pressure calculation along a hydraulic fracture, the weak form of the fluid mass balance equation (Rungamornrat et al. 2005; Segura and Carol 2008; Chen 2013) is applied to calculate the hydraulic pressure along the fracture and is presented as Eq. 4.

$$\int_L \frac{\Delta w}{\Delta t} N_i(x)dx + \int_L q_L(t) N_i(x)dx = \frac{1}{12\mu}\int_0^L \frac{\partial}{\partial x}\left(w^3 \frac{\partial P}{\partial x}\right) N_i(x)dx \tag{4}$$

where w is the fracture aperture, t is the time, L is the fracture length, q_L is the fluid leak-off rate from the fracture to the surrounding rocks, μ is the fluid dynamic viscosity, and P is the fluid pressure. Boundary conditions are applied at each end of the fracture for fluid injection at the wellbore and zero fluid pressure. The boundary conditions are summarized as in Eqs. 5 and 6.

$$\frac{1}{12\mu}\left(w^3 \frac{\partial P}{\partial x}\right) N_i(x)\Big|_{well} = Q_i N_1(0) \tag{5}$$

$$P\big|_{tip} = 0 \tag{6}$$

where Q_i is the fluid injection rate, and $P|_{tip}$ is the zero-fluid pressure at the tip.

Once the fluid pressure along the fracture is estimated, it is then applied to the global force vector, and the modified force vector is used by the XFEM program to calculating the trial solution of the fracture aperture. The entire process is repeated for each time step, and the resulting two trial solutions (w_k and $w_{k+1/2}$) in terms of the fracture opening are compared with each other to update the solution as in Eq. 7.

$$w_{k+1} = (1-\alpha) w_k + \alpha w_{k+1/2} \quad (7)$$

where α is the convergence coefficient of the Picard iteration. Convergence is determined by comparing the relative error between w_k and w_{k+1} for all elements along the fracture as shown in Eq. 8.

$$\varepsilon_{cvg} = \frac{\sum |w_{k+1} - w_k|}{\sum |w_k|} \quad (8)$$

Iterations stop when the relative error, ε_{cvg} is less than 10^{-6}, at which time the fracture aperture and fluid pressure are taken as the converged solution.

To demonstrate the coupled XFEM model, an example study is demonstrated as in Fig. 4. The initial fracture half-length is 1.5m, and a constant fracture propagation (L_{prop} = 0.2m) is added at the previous tip location when K_I exceeds K_{IC}, which is set to 5,000 Pa-m$^{1/2}$. For this example, 5 propagation steps are considered.

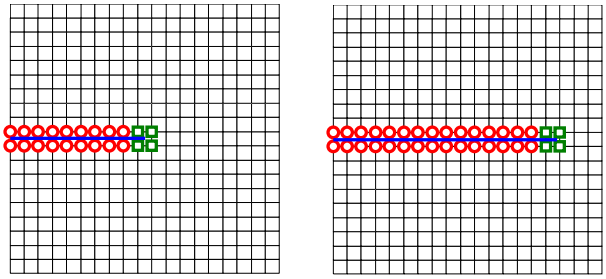

Figure 4. Enriched node selections (left: before propagations, right: after propagations)

As the fracture tip moves to the right, Branch function enriched nodes are switched to Heaviside enriched nodes, and the nodes around the new fracture tip are in turn enriched by Branch functions (See Fig. 4).

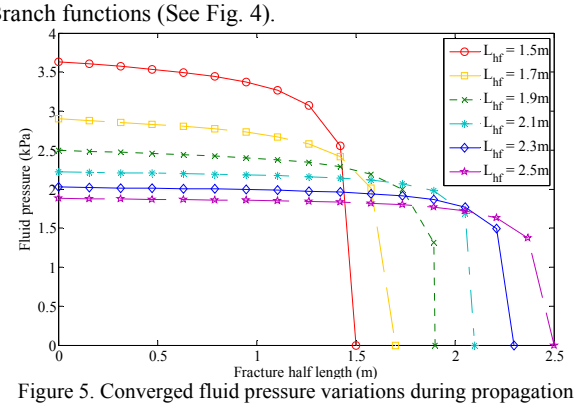

Figure 5. Converged fluid pressure variations during propagation

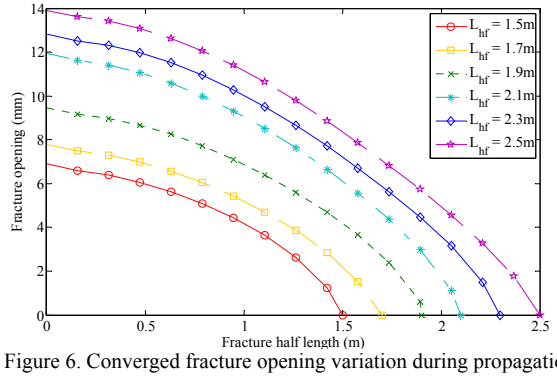

Figure 6. Converged fracture opening variation during propagation

Fig. 5 shows the fluid pressure variations for each fracture propagation step. Because SIF is a function of fracture length, longer fracture lengths yield relatively lower hydraulic pressure levels along the fracture. Furthermore, the converged fracture aperture distributions are shown in Fig. 6. As the fracture length increases, the aperture variation increases almost proportionally. The fluid pressure and fracture aperture changes are compared to the classical KGD model, and both results present good agreement.

3 PRESSURE LEAK-OFF TEST DURING HYDRAULIC AND NATURAL FRACTURE INTERACTIONS

In this section, a series of the pressure leak-off test is performed using the hydro-mechanical coupled XFEM program. If the fluid pressure yields enough stress concentration at the tip, the fracture propagates and creates additional fracture volume so that the fluid pressure decreases.

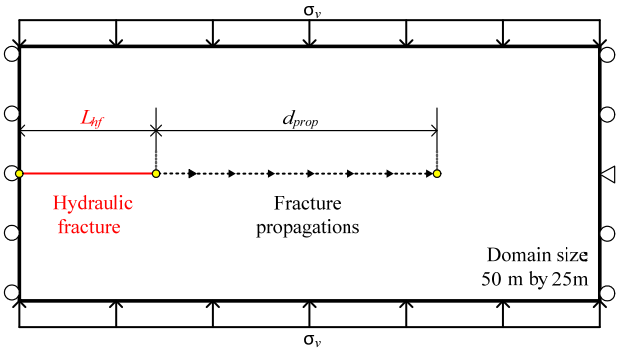

Figure 7. Schematics of pressure leak-off test without natural fracture

An example model is designed without natural fractures as in Fig. 7 for the pressure leak-off data comparisons. Constant elastic material properties (Young's modulus, E and Poisson's ratio, v) are applied to the entire domain, and a hydraulic fracture is aligned horizontally at the middle of the domain. The uniform compressive stress is applied on the upper and bottom boundaries, and a pin and multiple rollers are applied on both side to constrain lateral movement of the formation. All the rock and fluid properties are from field studies and related simulation work (e.g. Dahi, 2009 and Youn, 2016) and summarized in Table 1.

Table 1. Rock and Fluid properties for the example study

E	v	K_{IC}	σ_v	Q_i	M
10MPa	0.3	1MPa-m$^{1/2}$	50MPa	10m^3/min	1cp

Firstly, pressure leak-off test data is generated with variable initial fracture half lengths, L_{hf} (from 2m to 5m), and the result is summarized in Fig. 8.

During the initial fluid injection, the fluid pressure increases linearly to the formation breakdown pressure (FBP). Later the pressure gradually drops due to the fracture propagation. The initial fracture length greatly affects both the FBP and the initial pumping time needed to initiate fracture propagation. When a longer initial fracture is assumed, it takes more time to fill the greater fracture volume, although less fluid pressure is required to initiate fracture propagation. Once fracture propagations start, all the fluid pressure curves rapidly converge and present similar pressure levels regardless of the initial fracture length.

In the second example, a horizontal natural fracture is added into the domain collinear with the initial hydraulic fracturing trajectory as presented in Fig. 9. The hydraulic fracture initial length and the distance, d, between the hydraulic and natural fractures are set to 2m and 5m, respectively. To add different fracture volume increases, the natural fracture length, L_{nf} varies

from 2m to 5m as well. During initial pumping time, the pressure variations are almost identical (See Fig. 10). After around 0.15 minute from the start of fluid pumping, the hydraulic fracture contacts the natural fracture. The increased fracture volume clearly results in a significant decrease in the fluid pressure, and the longer fracture results in greater pressure reduction. Note that the dropped fluid pressure gradually approaches the pressure decline curve of the non-natural fracture case with time.

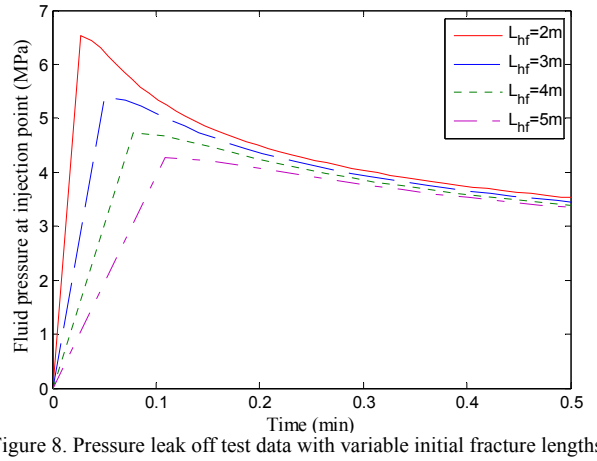

Figure 8. Pressure leak off test data with variable initial fracture lengths

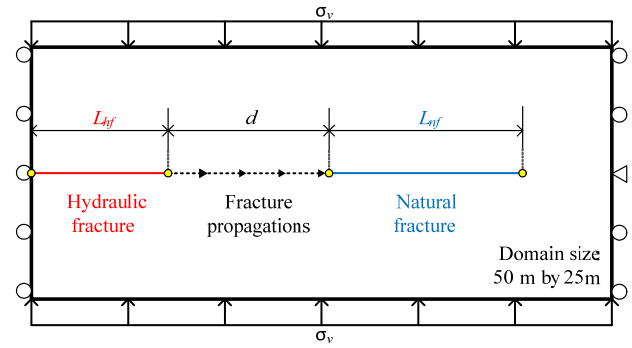

Figure 9. Schematics of pressure leak-off test with a natural fracture

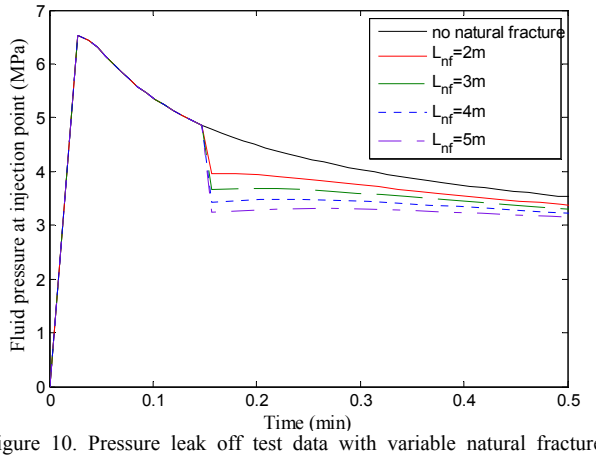

Figure 10. Pressure leak off test data with variable natural fracture lengths when d=5m

Lastly, the distance between the hydraulic and natural fracture, d was changed from 5m to 8m, while the size of both fractures was kept constant (4m). A dramatic decrease of the pressure was observed when the hydraulic fracture coalescence with the natural fracture (See Fig 11). If the distance increases, the fracture propagation takes longer to reach the natural fracture, causing the sudden decrease in fluid pressure at different times.

All these observations regarding pressure leak-off confirm that the pressure reduction computed at the injection point has a great potential to monitor and check the progress of the hydraulic fracturing process. The pressure leak off test results can present different pressure dropping tendencies when natural fracture sizes and locations vary.

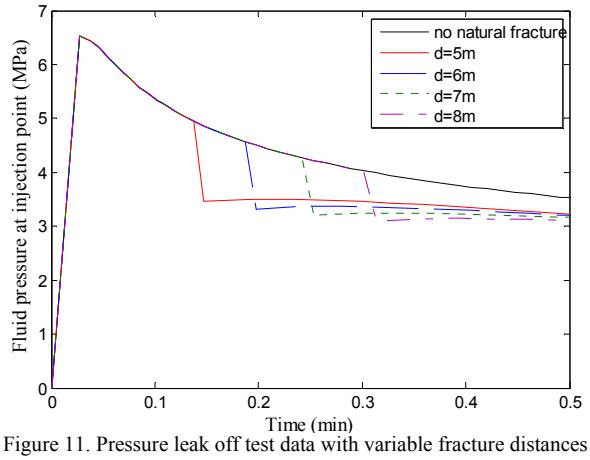

Figure 11. Pressure leak off test data with variable fracture distances

4 CONCLUSION

A sequential coupling scheme with Picard iteration was integrated to the XFEM program to the analyze hydraulic fracturing procedure. After validating the model with the KGD, the coupled XFEM was used to monitor the fluid bottomhole pressure variation during a pressure leak-off test, while a hydraulic fracture propagated and contacted pre-existing natural fractures. The pressure leak-off test analyses clearly demonstrated the pressure drop that occurs when a hydraulic fracture connects with a natural fracture, due to the sudden fracture volume increase. The fluid pressure variations at the injection point effectively indicates not only the progress of hydraulic fracture propagation but also the interactions with natural fractures.

5 REFERENCES

Youn, D.J. 2016. *Hydro-mechanical coupled simulation of hydraulic fracturing using the extended finite element method (XFEM)*. PhD Dissertation, Colorado School of Mines. Arthur Lakes Library.

Belytschko, T. and Black, T. 1999. Elastic crack growth in finite elements with minimal remeshing. *International Journal for Numerical Methods in Engineering*, *45*(5),601–620.

Moës, N., Dolbow, J., and Belytschko, T. 1999. A finite element method for crack growth without remeshing. *International Journal for Numerical Methods in Engineering*, 46(1),131–150.

Dahi. H. 2009. Analysis of hydraulic fracture propagation in fractured reservoirs: an improved model for the interaction between induced and natural fractures. University of Texas at Austin.

Khoei, A. R., and Vahab, M. 2014. A numerical contact algorithm in saturated porous media with the extended finite element method. *Computational Mechanics*, *54*(5),1089-1110.

Rungamornrat, J., Wheeler, M., and Mear, M. 2005. A Numerical Technique for Simulating Non-planar Evolution of Hydraulic Fractures. *In Proceedings of SPE Annual Technical Conference and Exhibition*, Society of Petroleum Engineers.

Segura, J. M., and Carol, I. 2008. Coupled HM analysis using zero-thickness interface elements with double nodes. Part I: Theoretical model. International Journal for Numerical and Analytical Methods in Geomechanics, *32*(18),2083–2101.

Chen, Z. 2013. *An ABAQUS Implementation of the XFEM for Hydraulic Fracture Problems*. Dr. Rob Jeffrey Ed., Effective and Sustainable Hydraulic Fracturing, InTech.